Thermodynamic Description of Inelastic Collisions in General Relativity

Jörg Hennig, Gernot Neugebauer

Theoretisch-Physikalisches Institut, Friedrich-Schiller-Universität Jena, Max-Wien-Platz 1, D-07743 Jena, Germany

J.Hennig@tpi.uni-jena.de

and

Marcus Ansorg

Max-Planck-Institut für Gravitationsphysik, Albert-Einstein-Institut, Am Mühlenberg 1, D-14476 Golm, Germany

marcus.ansorg@aei.mpg.de

ABSTRACT

We discuss head-on collisions of neutron stars and disks of dust ("galaxies") following the ideas of equilibrium thermodynamics, which compares equilibrium states and avoids the description of the dynamical transition processes between them. As an always present damping mechanism, gravitational emission results in final equilibrium states after the collision. In this paper we calculate selected final configurations from initial data of colliding stars and disks by making use of conservation laws and solving the Einstein equations. Comparing initial and final states, we can decide for which initial parameters two colliding neutron stars (non-rotating Fermi gas models) merge into a single neutron star and two rigidly rotating disks form again a final (differentially rotating) disk of dust. For the neutron star collision we find a maximal energy loss due to outgoing gravitational radiation of 2.3% of the initial mass while the corresponding efficiency for colliding disks has the much larger limit of 23.8%.

1. Introduction

Collisions of compact objects are an important source of gravitational radiation. Much effort has recently been made to develop numerical methods and codes describing and simulating the underlying hydrodynamical and gravitational phenomena. After the pioneering

work on numerical black hole evolutions by Eppley and Smarr in the 1970's [see e.g. Eppley (1975) and Smarr et al. (1976)], head-on collisions were re-investigated in the 1990's (Anninos et al. 1993, 1995, 1998) with good agreement between numerical and perturbation-theoretical results. Long-term-stable evolutions of black hole and neutron star collisions were successfully performed in the last two years (Sperhake et al. 2005; Fiske et al. 2005; Zlochower et al. 2005; Sperhake 2006; Löffler et al. 2006).

From a mathematical point of view collision processes are typical examples for initial-boundary problems. In particular, we will discuss head-on collisions of spheres and disks[1], see Fig. 1. Starting with bodies separated by a large ("infinite") distance we may model the initial situation by a quasi-equilibrium configuration of two isolated bodies. Corresponding solutions for spheres and (rigidly rotating) disks can be found in the literature, see e.g. Misner et al. (2002), Shapiro & Teukolsky (1983) and Neugebauer & Meinel (1993, 1994, 1995). The dynamical phase of the collision process is always accompanied by gravitational radiation. This damping mechanism results again in the formation of an equilibrium configuration after the collision. The rigorous mathematical description of the dynamical transition phase is difficult and requires extensive numerical investigations. However, interesting information about the collision can be obtained by comparing the initial and final (equilibrium) states. This thermodynamic idea avoids the analysis of the transition process and reduces the mathematical effort to solving the Einstein equations for the end products, which are stationary and axisymmetric in our case. The solution makes use of conservation laws which transfer data extracted from the initial configurations (spheres and disks before the collision) to the final configurations.

While the *initial* configurations are available the calculation of the *final* states is rather difficult. To cope with this problem for head-on colliding stars and disks, we will make use of two heuristic principles:

a) Perfect fluid configurations at rest are spherically symmetric. Hence, the end product of two head-on colliding spheres without angular momentum is again a sphere (a fluid ball or a Schwarzschild black hole).

b) Dust configurations are two-dimensional ("extremely flattened") and axisymmetric (with non-vanishing angular momentum). Consequently, the dust matter after a head-on collision of two disks of dust is again two-dimensional and axisymmetric (a compact disk, a disk surrounded by dust rings or a black hole surrounded by dust rings).

[1]Disk-like matter configurations play an important role in astrophysics, e.g. as models for galaxies, accretion disks or intermediate phases in the merger process of two neutron stars.

Though plausible, these principles have not been proved rigorously so far. For proofs under special assumptions see Beig & Simon (1992) and Lindblom & Masood-ul-Alam (1994).

As illustrated in Fig. 1 we will confine ourselves to two problems:

a) head-on collisions of two identical spheres (stars) merging into a single fluid ball and

b) head-on collisions of two identical disks of dust (galaxies) merging into a single disk.

It will turn out that our assumptions a) and b) together with the conservation of baryonic mass M_0 and angular momentum J define the final equilibrium configuration (balls/disks) uniquely. Obviously, both scenarios are based on restricted initial conditions. It is the goal of this paper to determine the appropriate subset of initial parameters (an "inappropriate" choice would lead to other final states as, e.g. to black holes or central bodies surrounded by rings) and to calculate the parameters of the end product (sphere/disk) as functions of this subset. Having solved this task we can determine the energy loss due to gravitational radiation, i.e. the efficiency η of the collision process.

In Sec. 2 we discuss, as introductory examples, the merger of two Schwarzschild stars and the collision of two (Fermi gas) neutron stars. Sec. 3 contains the main part of this paper which is dedicated to the investigation of disk collisions. These discussions are based on a novel solution of the Einstein equations. Here we continue the analysis of our paper (Hennig & Neugebauer 2006), in which we discussed the collisions of rigidly rotating disks of dust with parallel (or antiparallel) angular momenta under the simplifying assumption that the final disk be again a *rigidly* rotating (or rigidly counterrotating) disk of dust. This assumption can only be justified if friction processes between the disk rings provide for a constant angular velocity throughout the disk. This model seems to be somewhat artificial and unsuited to determining the contribution of gravitational radiation to the total energy loss. Interestingly, our present investigation will show that the frictional contribution to the total energy loss for colliding rigidly rotating disks is comparably small.

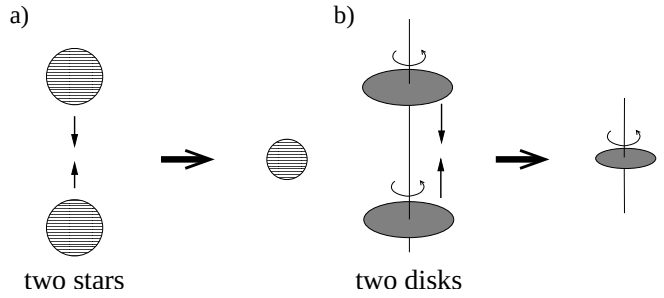

Fig. 1.— Model: collisions of spherically symmetric stars or rigidly rotating disks of dust

2. Star collisions

2.1. Introductory example: Schwarzschild stars

In order to demonstrate the method, we study the collision of two Schwarzschild stars, i.e. spherically symmetric perfect fluid stars with a constant mass density, $\mu =$ constant. Though not very realistic, this model illustrates the main steps of the method.

The matter of a Schwarzschild star is described by the perfect fluid energy-momentum tensor

$$T^{ij} = (\mu + p)u^i u^j + pg^{ij} \tag{1}$$

with the pressure

$$p(r) = \frac{\sqrt{1 - \frac{8\pi\mu}{3}r^2} - \sqrt{1 - \frac{8\pi\mu}{3}r_0^2}}{3\sqrt{1 - \frac{8\pi\mu}{3}r_0^2} - \sqrt{1 - \frac{8\pi\mu}{3}r^2}}\mu, \tag{2}$$

where u^i, r and r_0 are the four-velocity, the radial coordinate and the coordinate radius of the star, respectively. The interior Schwarzschild metric can be written as

$$\mathrm{d}s^2 = \frac{\mathrm{d}r^2}{1 - \frac{8\pi\mu}{3}r^2} + r^2(\mathrm{d}\vartheta^2 + \sin^2\vartheta\,\mathrm{d}\varphi^2) - \left(\frac{3}{2}\sqrt{1 - \frac{8\pi\mu}{3}r_0^2} - \frac{1}{2}\sqrt{1 - \frac{8\pi\mu}{3}r^2}\right)\mathrm{d}t^2, \tag{3}$$

and the exterior Schwarzschild solution is

$$\mathrm{d}s^2 = \frac{\mathrm{d}r^2}{1 - \frac{2M}{r}} + r^2\left(\mathrm{d}\vartheta^2 + \sin^2\vartheta\mathrm{d}\varphi^2\right) - \left(1 - \frac{2M}{r}\right)\mathrm{d}t^2. \tag{4}$$

Note that we use the normalized units where $c = 1$ for the speed of light and $G = 1$ for Newton's gravitational constant.

The gravitational mass M,

$$M = \frac{4\pi\mu}{3}r_0^3, \tag{5}$$

follows from the matching condition at the star's surface and the baryonic mass M_0 is given by

$$M_0 = \int\limits_{t=t_0} \mu u^t\sqrt{-g}\,\mathrm{d}r\mathrm{d}\vartheta\mathrm{d}\varphi = 4\pi\mu\int\limits_0^{r_0}\frac{r^2\mathrm{d}r}{\sqrt{1 - \frac{8\pi\mu}{3}r^2}}. \tag{6}$$

Now we apply these formulae to the head-on collision of two stars. Restricting ourselves to collisions of two identical Schwarzschild stars we assume, that the final star be again a Schwarzschild star and have the same mass density (e.g. nuclear matter density),

$$\tilde{\mu} = \mu, \tag{7}$$

where from now on tildes denote quantities after the collision.

The conservation of baryonic mass during the collision process,

$$\tilde{M}_0 = 2M_0, \tag{8}$$

allows one to calculate the parameters of the final star as a function of the initial parameters. With (5), (6) and (7) the conservation equation (8) can be written as

$$\arcsin\left(\sqrt{\frac{2M}{r_0}}\frac{\tilde{r}_0}{r_0}\right) - \sqrt{\frac{2M}{r_0}}\frac{\tilde{r}_0}{r_0}\sqrt{1-\frac{2M}{r_0}\frac{\tilde{r}_0^2}{r_0^2}} = 2\left(\arcsin\sqrt{\frac{2M}{r_0}} - \sqrt{\frac{2M}{r_0}}\sqrt{1-\frac{2M}{r_0}}\right), \tag{9}$$

i.e. the radius ratio $\tilde{r}_0/r_0$ is a function of the initial mass-radius ratio $2M/r_0$. From this ratio we obtain the efficiency η of conversion of mass into gravitational radiation,

$$\eta = 1 - \frac{\tilde{M}}{2M} = 1 - \frac{1}{2}\left(\frac{\tilde{r}_0}{r_0}\right)^3, \tag{10}$$

and the mass-radius ratio of the final star,

$$\frac{2\tilde{M}}{\tilde{r}_0} = \frac{2M}{r_0}\left(\frac{\tilde{r}_0}{r_0}\right)^2. \tag{11}$$

The resulting parameter relations are plotted in Fig. 2. For Schwarzschild stars the coordinate radius is restricted by the Buchdahl condition, i.e.

$$r_0 > \frac{9}{8}\times 2M, \quad \tilde{r}_0 > \frac{9}{8}\times 2\tilde{M}. \tag{12}$$

As a consequence, the first graph shows, that "relativistic" initial stars with $2M/r_0 > 0.6482\ldots$ cannot merge into a new Schwarzschild star with the same mass density μ. The "physical" parts of the parameter relations are shown as solid curves while the forbidden parts are dashed. According to the third graph the efficiency η cannot exceed a maximal value of $\eta_{\max} \approx 19.7\%$.

2.2. Neutron stars: Completely degenerate ideal Fermi gas

In order to extend the discussion of the previous section to a more realistic star model, we replace the equation of state $\mu =$ constant by the equation for a completely degenerate ideal Fermi gas of neutrons.

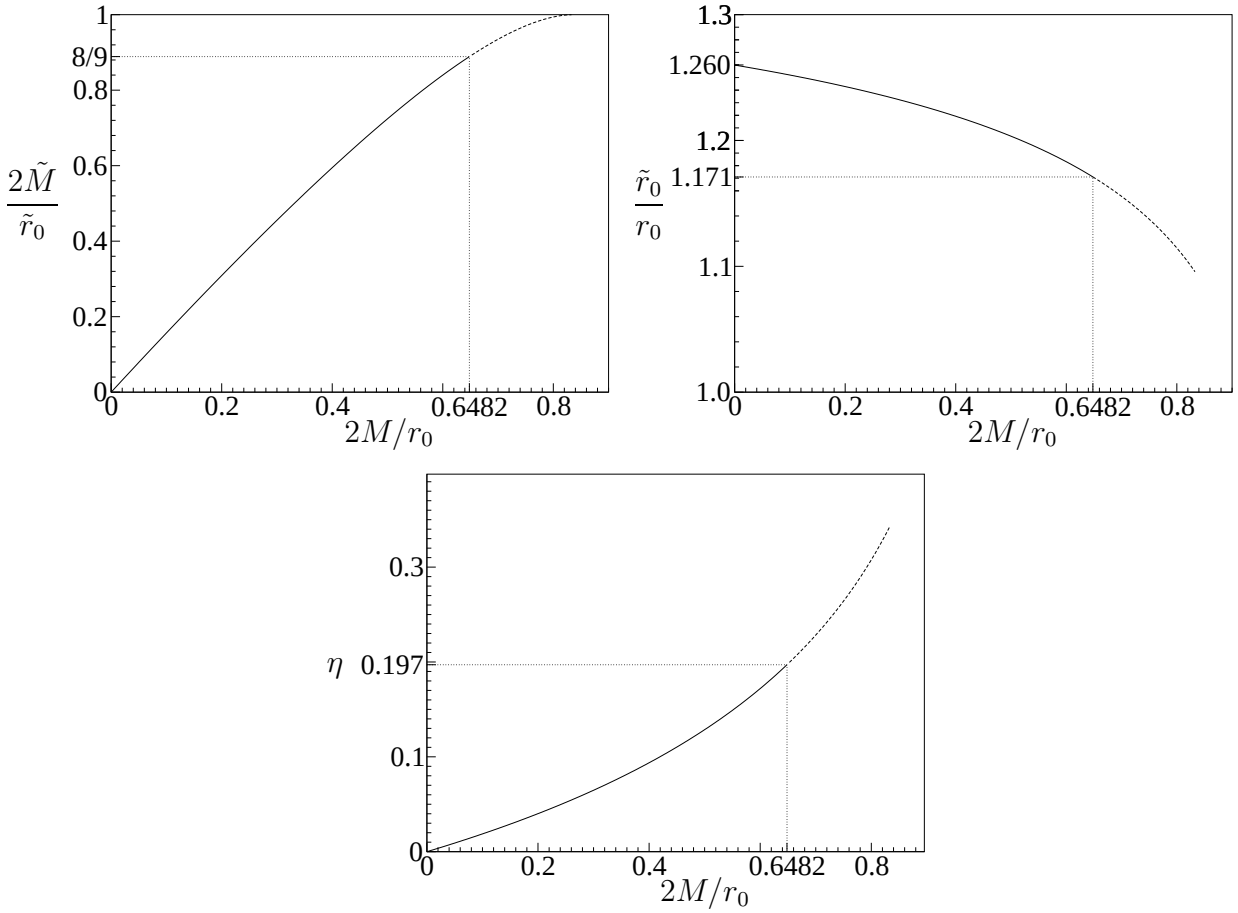

Fig. 2.— Parameter relations for colliding Schwarzschild stars: The final mass-radius ratio $2\tilde{M}/\tilde{r}_0$, the radius ratio $\tilde{r}_0/\tilde{r}$ and the efficiency η are plotted as functions of the initial mass-radius ratio $2M/r_0$. Dashed parts of the curves mark regions inaccessible due to the Buchdahl inequality $2\tilde{M}/\tilde{r}_0 < 8/9$.

The (interior) line element of a spherically symmetric star can be written as

$$\mathrm{d}s^2 = \mathrm{e}^{2\lambda(r)}\mathrm{d}r^2 + r^2(\mathrm{d}\vartheta^2 + \sin^2\vartheta\,\mathrm{d}\varphi^2) - \mathrm{e}^{2\nu(r)}\mathrm{d}t^2 \tag{13}$$

and the matter is again described by the ideal fluid energy-momentum tensor

$$T^{ij} = (\mu + p)u^i u^j + p g^{ij}. \tag{14}$$

With the definition of a new metric function $m(r)$ by

$$\mathrm{e}^{2\lambda(r)} = \frac{1}{1 - \frac{2m(r)}{r}}, \tag{15}$$

the field equations can be written in the TOV form, see e.g. Shapiro & Teukolsky (1983),

$$\frac{\mathrm{d}m}{\mathrm{d}r} = 4\pi r^2 \mu, \quad m(0) = 0 \tag{16}$$

$$\frac{\mathrm{d}p}{\mathrm{d}r} = -\frac{m}{r^2}\mu\left(1 + \frac{p}{\mu}\right)\left(1 + \frac{4\pi r^3 p}{m}\right)\left(1 - \frac{2m}{r}\right)^{-1}, \quad p(0) = p_\mathrm{c} \tag{17}$$

$$\frac{\mathrm{d}\nu}{\mathrm{d}r} = -\frac{1}{\mu}\frac{\mathrm{d}p}{\mathrm{d}r}\left(1 + \frac{p}{\mu}\right)^{-1}, \tag{18}$$

where p_c is the pressure in the center of the star.

We will solve these equations for the completely degenerate ideal fermi gas of neutrons with the equation of state [see e.g. Shapiro & Teukolsky (1983)]

$$p = c_1 f(x), \quad \rho = c_2 x^3, \quad \mu = \rho + c_1 g(x), \tag{19}$$

where

$$f(x) = x(2x^2 - 3)\sqrt{1 + x^2} + 3\ln(x + \sqrt{1 + x^2}), \tag{20}$$

$$g(x) = 8x^3(\sqrt{1 + x^2} - 1) - f(x), \tag{21}$$

$$c_1 = \frac{\pi m_\mathrm{n}^4}{3h^3}, \quad c_2 = \frac{8\pi m_\mathrm{n}^4}{3h^3} \tag{22}$$

with the neutron mass $m_\mathrm{n} = 1.6749286 \times 10^{27}\,\mathrm{kg}$ and Planck's constant $h = 6.626076 \times 10^{-34}\,\mathrm{Js}$. By solving the TOV equations (16) and (17) with the equation of state (19) for a sequence of values of the central density one can calculate the corresponding radii of the stars as the first zero r_0 of $p(r)$, their gravitational mass from $M = m(r_0)$, and their baryonic mass as

$$M_0 = 4\pi \int_0^{r_0} \frac{\rho(r) r^2 \mathrm{d}r}{\sqrt{1 - \frac{2m(r)}{r}}}. \tag{23}$$

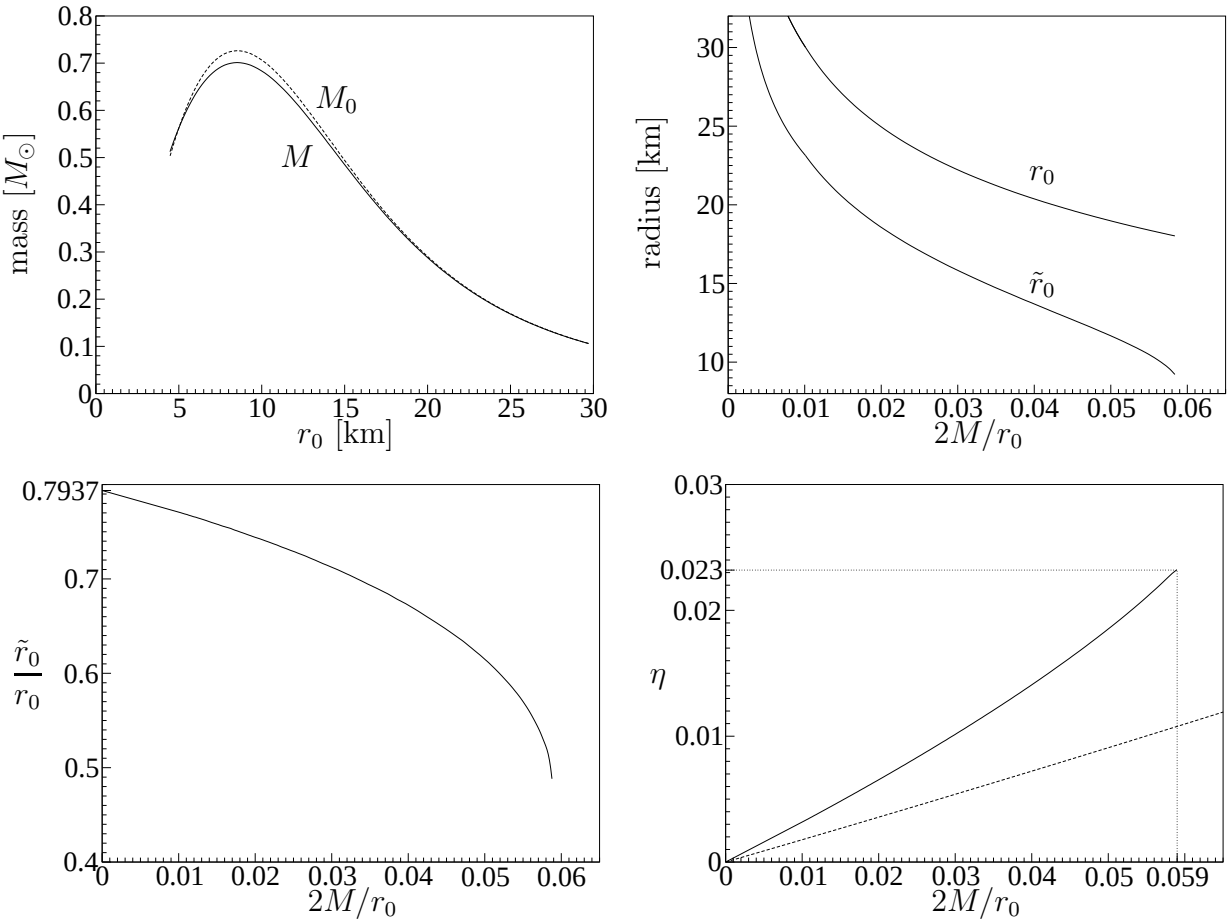

Fig. 3.— Parameter relations for the collisions of neutron stars made up of degenerate neutrons [cf. (19)]. First picture: mass-radius relations for the baryonic mass M_0 and the gravitational mass M. Second picture: initial radius r_0 and final radius $\tilde{r}_0$ as functions of the mass-radius ratio $2M/r_0$. Third picture: change of the coordinate radius. Fourth picture: efficiency η compared to the efficiency of the collision of Schwarzschild stars (dashed curve).

The resulting mass-radius relations are shown in the first graph of Fig. 3.

Again the baryonic mass is an invariant of the collision, i.e.

$$\tilde{M}_0 = 2M_0 \tag{24}$$

for the collision of two identical initial stars. This equation has to be analysed together with the mass-radius relations. (Thereby we take into account only stars in the monotonic decreasing part of the mass-radius relation $M_0(r_0)$.) The resulting parameter relations are shown in the remaining plots of Fig. 3. For the maximum of the efficiency one finds $\eta_{\max} \approx 2.3\%$, i.e. a comparably small value in view of the maximal efficiency $\eta_{\max} \approx 19.7\%$ for collisions of Schwarzschild stars. The reason is the relatively small maximal mass of $M_{\max} \approx 0.7M_\odot$ permitted by the equation of state (19) that excludes highly relativistic values for the mass-radius ratio $2M/r_0$. However, compared to Schwarzschild stars with the same parameter $2M/r_0$ the collisions of neutron stars are more efficient, cf. the last graph in Fig. 3.

Another difference is the change of the coordinate radii. While two Schwarzschild stars merge into a Schwarzschild star with a coordinate radius bigger than the initial radius, $\tilde{r}_0/r_0 > 1$ (cf. Fig. 2), the resulting neutron star is smaller than the initial neutron stars, $\tilde{r}_0/r_0 < 1$ (cf. Fig. 3).

3. Disk collisions

Collisions of disks of dust require more effort. In particular, the discussion of the final equilibrium state is based on a solution of a free boundary value problem to the Einstein equations. At the first glance, the conservation laws for baryonic mass and angular momentum are not sufficient to formulate a complete set of boundary conditions for the configuration after the collision. However, we may replace the global conservation laws, as used in Sec. 2, by local ones. Due to the geodesic motion of dust particles, the baryonic mass and the angular momentum of each of the rings forming the disk are conserved separately, see Fig. 5. Using such *local* conservation laws we will be able to solve (numerically) the boundary value problem for the final state after the head-on collision of two aligned rigidly rotating disks of dust with parallel angular momenta, cf. Fig. 1.

3.1. Initial disks: Rigidly rotating disks of dust

The free boundary value problem for the relativistic rigidly rotating disk of dust (RR disk) was discussed by Bardeen and Wagoner (1969, 1971) using approximation methods and analytically solved in terms of ultraelliptic theta functions by Neugebauer and Meinel (1993, 1994, 1995) using the Inverse Scattering Method. The line element of the stationary (Killing vector: ξ^i) and axisymmetric (Killing vector: η^i) space-time may be written in the Weyl-Lewis-Papapetrou standard form

$$\mathrm{d}s^2 = \mathrm{e}^{-2U}[\mathrm{e}^{2k}(\mathrm{d}\rho^2 + \mathrm{d}\zeta^2) + \rho^2\mathrm{d}\varphi^2] - \mathrm{e}^{2U}(\mathrm{d}t + a\mathrm{d}\varphi)^2, \quad \xi^i = \delta^i_t, \quad \eta^i = \delta^i_\varphi, \tag{25}$$

where the metric potentials $U = U(\rho, \zeta)$, $k = k(\rho, \zeta)$ and $a = a(\rho, \zeta)$ are given in terms of ultraelliptic functions.

The matter of the disk of dust is described by the energy-momentum tensor

$$T^{ij} = \varepsilon(\rho)\delta(\zeta)u^i u^j, \tag{26}$$

where $\varepsilon(\rho)\delta(\zeta)$ is the mass density with $\delta(\zeta)$ as Dirac's δ-distribution. Due to the symmetries, the four-velocity of the dust particles is a linear combination of the two killing vectors,

$$u^i = \mathrm{e}^{-V_0}(\xi^i + \Omega_0\eta^i), \quad u^i u_i = -1, \tag{27}$$

whence

$$(\xi^i + \Omega_0\eta^i)(\xi_i + \Omega_0\eta_i) = -\mathrm{e}^{2V_0}, \tag{28}$$

where Ω_0 is the angular velocity of the particles forming the disk and V_0 is a redshift parameter. Rigid rotation means $\Omega_0 =$ constant in the disk. Since dust particles move geodesically this assumption implies $V_0 =$ constant in the disk. Hence, the boundary condition (28) and as a consequence the RR disk solution contains two constant parameters. Alternatively to Ω_0 and V_0, we may choose the coordinate radius ρ_0 of the disk and a centrifugal parameter $\mu = 2\Omega_0^2\rho_0^2\mathrm{e}^{-2V_0}$ [$\mu \to 0$ turns out to be the Newtonian limit and $\mu \to 4.62966\ldots$ the ultra-relativistic limit, where the disk approaches the extreme Kerr black hole, cf. Neugebauer & Meinel (1994) and Neugebauer et al. (1996) for these and further properties].

3.2. Final disk: Differentially rotating disk of dust

Dust particles interact by gravitational forces alone. In general, the collision of rigidly rotating disks of dust will lead to a final disk with non-rigid (differential) rotation. To enforce rigid rotation one has to involve some additional friction between the rings of the disk as

discussed in detail in a previous paper (Hennig & Neugebauer 2006). A brief summary of those considerations will be given in the next subsection.

After that, we will see that the local conservation of baryonic mass and angular momentum is sufficient to calculate the final differentially rotating disk (numerically). Differentially rotating disks with arbitrary rotation law have already been studied (Ansorg & Meinel 2000; Ansorg 2001). The point made here is that we are able to formulate a physically motivated rotation law as a result of a collision process.

3.2.1. Formation of rigidly rotating disks

For the formation of an RR disk from two colliding RR disks the conservation equations for baryonic mass and angular momentum,

$$\tilde{M}_0 = 2M_0, \quad \tilde{J} = 2J, \tag{29}$$

are sufficient to calculate the parameters of the final disks as functions of the initial parameters. These equations and the explicit formulae for the gravitational mass M, the baryonic mass M_0 and the angular momentum J of the RR disk allowed us to calculate the efficiency $\eta^{\mathrm{RR}} = 1 - \tilde{M}/2M$ as a function of the initial centrifugal parameter μ, cf. Fig. 4. It should be emphasized once again, that this efficiency measures the total energy loss including friction. Therefore η is only an *upper limit* for the energy of the gravitational emission. We obtained a maximal value of $\eta^{\mathrm{RR}}_{\mathrm{max}} \approx 23.8\%$ (Hennig & Neugebauer 2006).

Furthermore, it turned out that the formation of RR disks from two colliding RR disks is only possible for a rather restricted interval $0 < \mu < 1.954\ldots$ of the initial centrifugal parameter μ. If μ exceeds this limit, the collision must lead to other final states, e.g. black holes or black holes surrounded by matter rings.

3.2.2. Local conservation equations

We now turn to the main goal of this paper and analyse the formation of a disk of dust under the influence of gravitational forces as the only form of interaction. In this way we may separate gravitational damping due to the emission of gravitational waves from frictional processes in the material.

We may interpret a disk of dust as a superposition of infinitesimally thin dust rings. Considering the geodesic motion of a single mass element, one can show that for corresponding rings in the two initial disks (see Fig. 5) the baryonic mass and the angular momentum

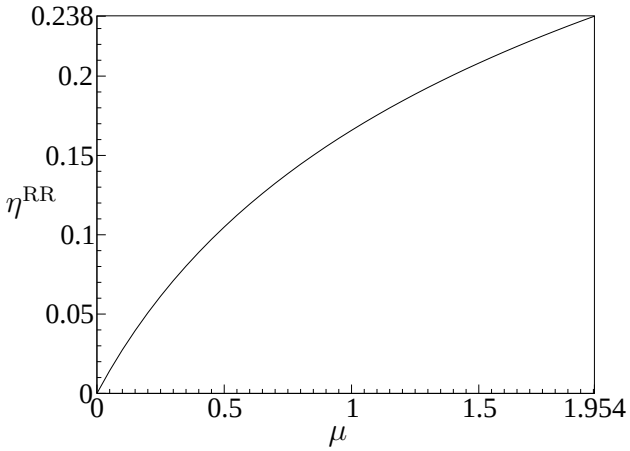

Fig. 4.— The efficiency η_{RR} for the formation of an RR disk from two initial RR disks as a function of the centrifugal parameter μ of the initial disks. η^{RR} is an upper limit for the energy loss due to gravitational radiation.

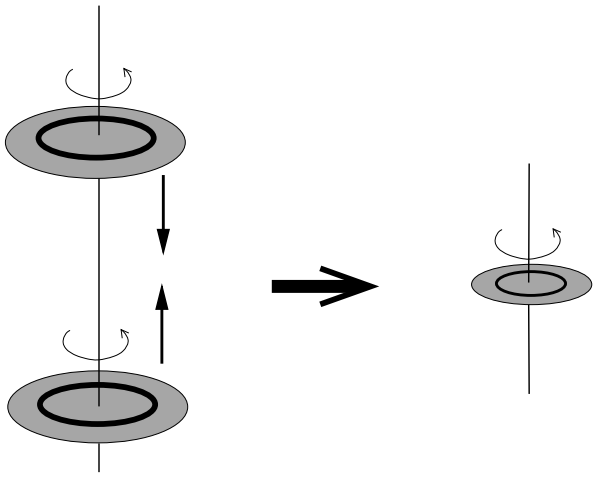

Fig. 5.— Illustration of the local conservation equations. Two corresponding rings of the initial disks merge into a ring in the final disk. The baryonic mass $\mathrm{d}M_0$ and the angular momentum $\mathrm{d}J$ of these rings are conserved.

are conserved,

$$\mathrm{d}\tilde{M}_0 = 2\mathrm{d}M, \quad \mathrm{d}\tilde{J} = 2\mathrm{d}J, \tag{30}$$

i.e. the baryonic masses $\mathrm{d}M_0$ and the angular momenta $\mathrm{d}J$ of the rings with radius ρ, taking up the interval $[\rho, \rho + \mathrm{d}\rho]$, in each of the two initial disks sum up to $\mathrm{d}\tilde{M}_0 = 2\mathrm{d}M_0$ and $\mathrm{d}\tilde{J} = 2\mathrm{d}J$ of the corresponding ring in the final disk (with radius $\tilde{\rho}$, taking up the interval $[\tilde{\rho}, \tilde{\rho} + \mathrm{d}\tilde{\rho}]$), cf. Fig. 5.

Eq. (30) provides us with a subset of the boundary conditions to be discussed in the next subsection. It will turn out that these conditions, together with conditions resulting from the field equations, determine a unique solution of the Einstein equations describing a final disk with differential rotation (DR disk) as the end product of the collision process.

3.2.3. Boundary value problem for the final DR disk

The line element (25), which may also be used to describe any axisymmetric and stationary *differentially* rotating disk, can be reformulated to give

$$\mathrm{d}\tilde{s}^2 = \mathrm{e}^{2\tilde{\kappa}}(\mathrm{d}\tilde{\rho}^2 + \mathrm{d}\tilde{\zeta}^2) + \tilde{\rho}^2\mathrm{e}^{-2\tilde{\nu}}(\mathrm{d}\tilde{\varphi} - \tilde{\omega}\mathrm{d}\tilde{t})^2 - \mathrm{e}^{2\tilde{\nu}}\mathrm{d}\tilde{t}^2, \tag{31}$$

where the usage of the functions $\tilde{\kappa}$, $\tilde{\nu}$ and $\tilde{\omega}$ [instead of $\tilde{U}$, $\tilde{k}$ and $\tilde{a}$ as in (25)] avoids numerical issues with ergospheres (where $\mathrm{e}^{2\tilde{U}} < 0$). According to (26) the energy-momentum tensor is

$$\tilde{T}^{ij} = \tilde{\varepsilon}(\tilde{\rho})\delta(\tilde{\zeta})\tilde{u}^i\tilde{u}^j \tag{32}$$

and the four-velocity is again [cf. (27)] a linear combination of the killing vectors,

$$\tilde{u}^i = \mathrm{e}^{-\tilde{V}}(\tilde{\xi}^i + \tilde{\Omega}\tilde{\eta}^i), \tag{33}$$

where $\tilde{V} = \tilde{V}(\tilde{\rho})$ and $\tilde{\Omega} = \tilde{\Omega}(\tilde{\rho})$ are functions of $\tilde{\rho}$ [constancy of $\tilde{V}$ and $\tilde{\Omega}$ defines rigid rotation, cf. (27)].[2]

The vacuum field equations for $\tilde{\nu}$ and $\tilde{\omega}$ are [cf. Bardeen (1973)]

$$\triangle_1\,\tilde{\nu} = \frac{\tilde{\rho}^2}{2}\mathrm{e}^{-4\tilde{\nu}}(\tilde{\omega}_{,\tilde{\rho}}^{\ 2} + \tilde{\omega}_{,\tilde{\zeta}}^{\ 2}), \quad \triangle_3\tilde{\omega} = 4(\tilde{\nu}_{,\tilde{\rho}}\tilde{\omega}_{,\tilde{\rho}} + \tilde{\nu}_{,\tilde{\zeta}}\tilde{\omega}_{,\tilde{\zeta}}), \tag{34}$$

with

$$\triangle_n := \partial_{\tilde{\rho}}^2 + \partial_{\tilde{\zeta}}^2 + \frac{n}{\tilde{\rho}}\partial_{\tilde{\rho}}. \tag{35}$$

[2] All quantities of the final DR disk are tilded.

The matter appears only in the boundary conditions along the disk ($\tilde{\zeta}=0$, $\tilde{\rho}<\tilde{\rho}_0$),

$$\tilde{\nu}_{,\tilde{\zeta}}\big|_{\tilde{\zeta}=0^+} = 2\pi\tilde{\sigma}\frac{1+\tilde{v}^2}{1-\tilde{v}^2}, \tag{36}$$

$$\tilde{\omega}_{,\tilde{\zeta}}\big|_{\tilde{\zeta}=0^+} = -8\pi\tilde{\sigma}\frac{\tilde{\Omega}-\tilde{\omega}}{1-\tilde{v}^2}, \tag{37}$$

$$\tilde{\rho}(\tilde{\Omega}-\tilde{\omega})^2 = (1+\tilde{v}^2)\mathrm{e}^{4\tilde{\nu}}\tilde{\nu}_{,\tilde{\rho}} + \tilde{\rho}^2(\tilde{\Omega}-\tilde{\omega})\tilde{\omega}_{,\tilde{\rho}}, \tag{38}$$

where

$$\tilde{v} := \tilde{\rho}\mathrm{e}^{-2\tilde{\nu}}(\tilde{\Omega}-\tilde{\omega}), \quad \tilde{\sigma} := \tilde{\varepsilon}\mathrm{e}^{2\tilde{\kappa}}. \tag{39}$$

As already mentioned, the local conservation equations (30) of the previous subsection lead to additional boundary conditions along the disk. From $\mathrm{d}\tilde{M}_0 = 2\mathrm{d}M_0$ with $\mathrm{d}M_0 = 2\pi\sigma\mathrm{e}^{-V_0}\rho\mathrm{d}\rho$ and $\mathrm{d}\tilde{M}_0 = 2\pi\tilde{\sigma}\mathrm{e}^{-\tilde{V}}\tilde{\rho}\mathrm{d}\tilde{\rho}$ we obtain

$$\tilde{\sigma} = 2\sigma\frac{\rho\mathrm{e}^{V_0}}{\tilde{\rho}\mathrm{e}^{\tilde{V}}}\frac{\mathrm{d}\rho}{\mathrm{d}\tilde{\rho}}. \tag{40}$$

Likewise, $\mathrm{d}\tilde{J} = 2\mathrm{d}J$ with $\mathrm{d}J = 2\pi\sigma\mathrm{e}^{-V_0}u^i\eta_i\rho\mathrm{d}\rho$ and $\mathrm{d}\tilde{J} = 2\pi\tilde{\sigma}\mathrm{e}^{-\tilde{V}}\tilde{u}^i\tilde{\eta}_i\tilde{\rho}\mathrm{d}\tilde{\rho}$, $u^i\eta_i = \rho v\mathrm{e}^{-V_0}$ and $\tilde{u}^i\tilde{\eta}_i = \tilde{\rho}\tilde{v}\mathrm{e}^{-\tilde{V}}$ leads to

$$\tilde{\rho}\tilde{v}\mathrm{e}^{-\tilde{V}} = \rho v\mathrm{e}^{-V_0}. \tag{41}$$

The function $\tilde{V}(\tilde{\rho})$ can be calculated from $\tilde{u}^i\tilde{u}_i = -1$,

$$\mathrm{e}^{2\tilde{V}} = (1-\tilde{v}^2)\mathrm{e}^{2\tilde{\nu}}. \tag{42}$$

The remaining boundary conditions describe the behaviour at infinity, where the metric approaches the flat Minkowski metric,

$$\tilde{\kappa} = \tilde{\nu} = \tilde{\omega} = 0, \tag{43}$$

and in the plane $\tilde{\zeta}=0$ outside the disk ($\tilde{\rho}>\tilde{\rho}_0$), where (36) and (37) lead to vanishing normal derivatives,

$$\tilde{\nu}_{,\tilde{\zeta}}\big|_{\tilde{\zeta}=0^+} = 0, \quad \tilde{\omega}_{,\tilde{\zeta}}\big|_{\tilde{\zeta}=0^+} = 0. \tag{44}$$

In addition we have to ensure regularity along the axis of symmetry $\tilde{\rho}=0$.

Eqs. (34), (36)-(38) and (40), (41) form a complete set of equations to determine the unknown functions uniquely: There are two two-dimensional functions, $\tilde{\nu}(\tilde{\rho},\tilde{\zeta})$ and $\tilde{\omega}(\tilde{\rho},\tilde{\zeta})$, which have to satisfy the two elliptic equations (34) with the boundary conditions (36) and (37), and three additional one-dimensional functions in the disk, $\tilde{\Omega}(\tilde{\rho})$, $\tilde{\sigma}(\tilde{\rho})$, $\rho(\tilde{\rho})$, which have to obey the three boundary conditions (38), (40) and (41). (The metric function $\tilde{\kappa}$ can be calculated by a line integral afterwards, but is not needed for the computation of the efficiency η in our collision scenario.)

3.2.4. Numerical method

In order to prepare numerical investigations we will map the region $0 \le \tilde{\rho} \le \infty$, $0 \le \tilde{\zeta} \le \infty$ to a unit square thus reaching a compactification of infinity, cf. Fig. 6. (Due to the reflection symmetry with respect to the plane $\tilde{\zeta} = 0$ we can restrict ourselves to the region $\tilde{\zeta} \ge 0$.) To do this we introduce in a first step elliptical coordinates

$$\tilde{\rho} = \sqrt{(1+\xi^2)(1-\eta^2)}, \quad \tilde{\zeta} = \xi\eta, \quad \xi \in [0,\infty], \quad \eta \in [0,1] \tag{45}$$

(without loss of generality, we may choose units where $\tilde{\rho}_0 = 1$). In a second step we stretch the coordinates by the transformation

$$\xi = \cot\left(\frac{\pi}{2}s\right), \quad \eta = \sqrt{1-t}, \quad s \in [0,1], \quad t \in [0,1]. \tag{46}$$

The coordinates s and t form a unit square with the following boundaries,

$$\begin{aligned} s = 0: &\quad \infty \\ s = 1: &\quad \text{disk},\ \tilde{\rho} \le 1,\ \tilde{\zeta} = 0 \\ t = 0: &\quad \text{axis of symmetry},\ \tilde{\rho} = 0 \\ t = 1: &\quad \text{disk plane } \mathcal{E} \text{ outside the matter},\ \tilde{\rho} > 1,\ \tilde{\zeta} = 0. \end{aligned}$$

The unknown functions in the boundary value problem are analytic functions in this square (as is known for the case of Maclaurin disks or the RR disks). Hence, it is convenient to use spectral methods for the numerical solution of the boundary value problem. We expand the unknown potentials in terms of Chebyshev polynomials T_j to a predetermined order in the form

$$f(s,t) = \sum_{j,k} c_{jk} T_j(2s-1) T_k(2t-1) \quad \text{or} \quad f(t) = \sum_k c_k T_k(2t-1) \quad \text{(boundary)} \tag{47}$$

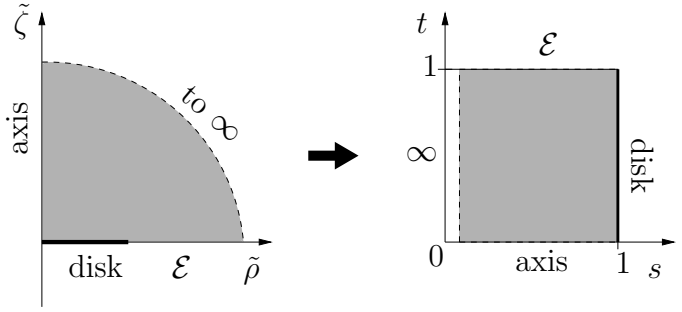

Fig. 6.— The coordinate transformation (45), (46) maps the part $\tilde{\zeta} \ge 0$ of the $\tilde{\rho}$-$\tilde{\zeta}$-plane to a unit square in the s-t-plane. $\mathcal{E}$ denotes the equatorial plane outside the disk, $\tilde{\zeta} = 0$, $\tilde{\rho} > \tilde{\rho}_0$.

and formulate the Einstein equations at the extrema of the Chebyshev polynomials. This leads to an algebraic system of equations for the Chebyshev coefficients (or, alternatively, for the values of the potentials at these points) that can be solved with the Newton-Raphson method. The iteration starts with an initial "guessed" solution (for example the Newtonian approximation, see Sec. 3.2.6 below).

The calculations show a decreasing accuracy of the numerical solution for increasingly large values of the initial parameter μ. The reason are large gradients of the metric potentials for strong relativistic DR disk which make the Chebyshev approximation more costly. To reach a better convergence we perform an additional coordinate transformation

$$s = \frac{\sinh(\delta \cdot \tilde{s})}{\sinh(\delta)} \tag{48}$$

introducing a new coordinate $\tilde{s}$, where δ is a suitably chosen parameter. As shown in Ansorg & Petroff (2005), this transformation smooths the gradients of the metric functions. The convergence is illustrated in Fig. 7.

3.2.5. Results

Using this numerical algorithm, we are able to solve the boundary value problem for the final DR disk. In particular, we could calculate, for each value of the initial parameter μ, all *metric coefficients* of this final disk. However, we will restrict ourselves to the discussion of the relations between the initial and final *parameters* and the *efficiency* of the collision process. In particular, we will compare the final DR disk with an RR disk having the same baryonic mass and angular momentum. The point made here is that such a rigidly rotating disk represents the state of "thermodynamic equilibrium" for disks of dust as the end point of their thermodynamic evolution. As sketched in Fig. 8, there are at least two possibilities for the formation of this final RR disk: The direct process (A) including friction from the beginning or the equivalent thermodynamic process (B) where, in a first step, a *differentially rotating* disk is formed (by gravitational damping alone, no friction) and, in a second step, the angular velocity becomes *constant* (due to friction). Note that baryonic mass and angular momentum are conserved in both processes. By comparing (A) and (B) we may extract the contribution of friction in scenario (A).

In the following discussion, tilded quantities, as before, belong to the final DR disk of scenario (B) in Fig. 8, a superscript "RR" denotes quantities of the final RR disk in scenario (A) and the centrifugal parameter μ without any additions characterizes the initial RR disks.

The rotation curve of the final DR disk, i.e. its (normalized) angular velocity $\tilde{\Omega}\tilde{\rho}_0$

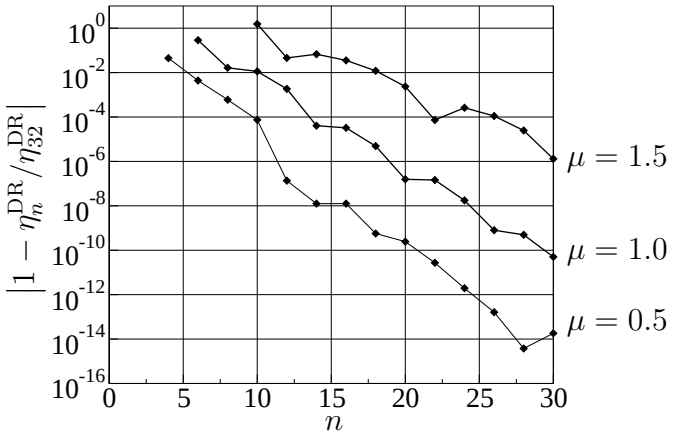

Fig. 7.— Convergence properties of the numerical code for the example η^{DR}. The values of the efficiency η^{DR} for different orders $n_s = n_t = n$ of the Chebyshev expansion are related to the order $n = 32$. The picture shows $\left|1-\eta_n^{\mathrm{DR}}/\eta_{32}^{\mathrm{DR}}\right|$ as function of n.

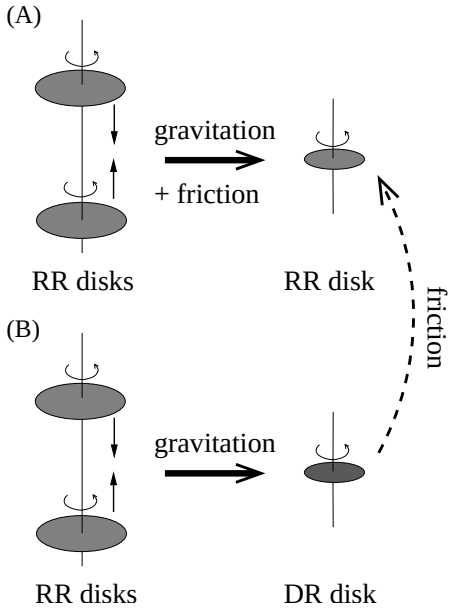

Fig. 8.— Two models for disk collisions:
(A) Under the influence of a small amount of friction, RR disks merge again into an RR disk. This scenario was discussed in Hennig & Neugebauer (2006), see Sec. 3.2.1.
(B) In the absence of friction, the same RR disks merge into a DR disk. Allowing for friction afterwards, the system would again arrive at the RR disk of scenario (A) after a sufficiently long time.

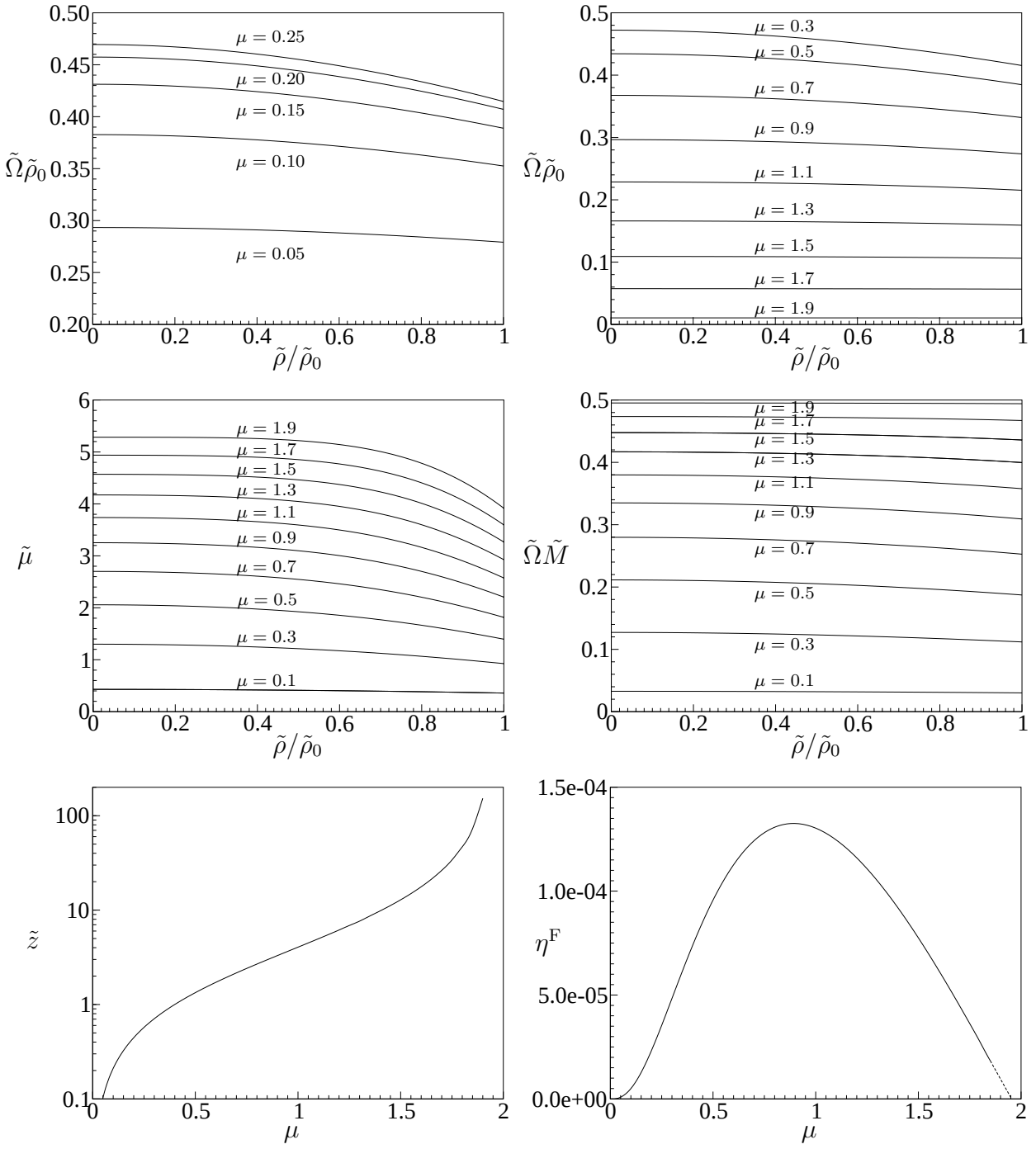

Fig. 9.— Parameter relations for the collision of RR disks. We performed numerical calculations for initial values of the centrifugal parameter μ in the invervall $[0, 1.9]$. The dotted part of the curve in the last graph is an extrapolation for larger μ. This extrapolation and the rapidly growing redshift in the second last graph indicate, that the initial parameter μ in scenario (B) is limited (approximately, or perhaps even exactly) to the same interval as in scenario (A), $0 < \mu < 1.954\ldots$, see Sec. 3.2.1.

as a function of the (normalized) radius $\tilde{\rho}/\tilde{\rho}_0$ is shown in the first two pictures of Fig. 9. For small parameters μ (post-Newtonian regime) the function $\tilde{\Omega}\tilde{\rho}_0$ is almost constant (first picture). Interestingly, strongly relativistic disks ($\mu \gtrsim 1.5$) show the same property (second picture). Moreover, $\tilde{\Omega}\tilde{\rho}_0$ tends to zero in the ultrarelativistic limit in analogy to the relation $\Omega^{\mathrm{RR}}\rho_0^{\mathrm{RR}} \to 0$ which holds for RR disks in the ultrarelativistic limit $\mu^{\mathrm{RR}} \to 4.62966\ldots$

The "centrifugal parameter" $\tilde{\mu} = 2\tilde{\Omega}^2\tilde{\rho}_0^2 \mathrm{e}^{-\tilde{V}} = \mu(\tilde{\rho})$ is shown in the third picture of Fig. 9. Like the angular velocity, $\tilde{\mu}$ is almost constant for small μ. For strongly relativistic DR disks, $\tilde{\mu}$ in the center of the disk exceeds the limit $\mu_{\max}^{\mathrm{RR}} = 4.62966\ldots$ of RR disks.

The fourth picture of Fig. 9 shows the quantity $\tilde{\Omega}\tilde{M}$ as a function of ρ/ρ_0. For strongly relativistic DR disks $\tilde{\Omega}\tilde{M}$ becomes constant and approaches the limit 0.5. On the other hand, this is a characteristic value for extreme Kerr black holes where $\Omega_{\mathrm{H}} M_{\mathrm{BH}} = 0.5$ (Ω_{H}: angular velocity of the horizon, M_{BH}: black hole mass). Indeed, one can show that there is a phase transition between RR disks and Kerr black holes (Bardeen & Wagoner 1971; Neugebauer & Meinel 1994). This inspires the conjecture that the DR disk exhibits the same phase transition. There is no obstacle for a (numerical) proof of this assumption in principle. To extend our present code to study the parametric collapse of the DR disk including the formation of a horizon we would have to follow the ideas of Bardeen and Wagoner (1971) who analysed this problem for the RR disks. However, such investigations are outside the scope of this paper.

The fifth picture of Fig. 9 shows the redshift $\tilde{z}$ for a photon emitted from the disk center as a function of the initial centrifugal parameter μ. For increasing values of μ (relativistic DR disks) $\tilde{z}$ grows rapidly.

An important result is the efficiency η^{DR} of the formation of DR disks which measures the amount of energy converted into gravitational radiation. The difference $\eta^{\mathrm{F}} = \eta^{\mathrm{RR}} - \eta^{\mathrm{DR}}$ as shown in the last graph of Fig. 9 compares this value with the efficiency η^{RR} of the RR disk forming process as sketched in scenario (A) of Fig. 8. Thereby, η^{F} is the part of energy lost due to friction during the formation of a final RR disk. We find $\eta^{\mathrm{F}} = \eta^{\mathrm{RR}} - \eta^{\mathrm{DR}} < 1.5 \times 10^{-4}$, i.e. the contribution of friction is extremely small, $\eta^{\mathrm{F}} \ll \eta^{\mathrm{RR}}$, such that the gravitational radiation dominates the collision process (A).

3.2.6. Analytical treatment of the Newtonian limit

Our numerical investigations have shown that the angular velocity of the final DR disk becomes closer and closer to a constant over the whole range of $\tilde{\rho}/\tilde{\rho}_0$ as the centrifugal parameter μ tends to zero (cf. the first picture of Fig. 9). This leads one to suspect that

a final disk with a *strictly* constant angular velocity will solve the boundary value problem as discussed in Sec. 3.2.3 in *Newtonian* theory. Interestingly, we can solve this problem analytically. This will now be demonstrated. Strictly speaking, there is no gravitational radiation in Newton's theory. However, this Newtonian boundary value problem can be seen as the limit of a sequence of relativistic collisions with decreasing μ, all reaching a final equilibrium state. Moreover, the Newtonian solution can be used as a starting point for the iterative calculation of the final relativistic DR disk.

Since the Newtonian limit of the RR disk is the Maclaurin disk we have to study the collision of two identical Maclaurin disks using the local conservation laws (30). The Newtonian potential $\tilde{U}$ of the final disk is a solution of the Poisson equation

$$\triangle \tilde{U} = 4\pi\tilde{\sigma}\delta(\zeta) \tag{49}$$

with the boundary condition

$$\tilde{U}_{,\tilde{\zeta}}\Big|_{\tilde{\zeta}=0+} = 2\pi\tilde{\sigma}, \tag{50}$$

where $\tilde{\sigma} = \tilde{\sigma}(\tilde{\rho})$ is the surface mass density of the final disk. With $\mathrm{d}M = 2\pi\sigma\mathrm{d}\rho$ and $\mathrm{d}J = \Omega\rho^2\mathrm{d}M$, Eq. (30) leads to the additional boundary conditions

$$\tilde{\sigma}(\tilde{\rho}) = 2\sigma(\rho)\frac{\rho}{\tilde{\rho}}\frac{\mathrm{d}\rho}{\mathrm{d}\tilde{\rho}}, \quad \tilde{\Omega}(\tilde{\rho})\tilde{\rho}^2 = \Omega_0\rho^2. \tag{51}$$

The initial surface mass density of the Maclaurin disk is

$$\sigma(\rho) = \frac{3M}{2\pi\rho_0^2}\sqrt{1-\frac{\rho^2}{\rho_0^2}} \tag{52}$$

and the initial constant angular velocity Ω_0 is related to the initial mass by

$$\Omega_0^2 = \frac{3\pi M}{4\rho_0^3}. \tag{53}$$

Using these relations, together with the Euler equation

$$\tilde{U}_{,\tilde{\rho}}\Big|_{\tilde{\zeta}=0} = \tilde{\Omega}^2(\tilde{\rho})\tilde{\rho}, \tag{54}$$

we find that a (rigidly rotating) Maclaurin disk with the parameters

$$\tilde{\Omega} = 4\Omega_0, \quad \tilde{\rho}_0 = \frac{1}{2}\rho_0 \tag{55}$$

indeed solves the boundary value problem.

colliding objects	$\eta_{\max}$
Schwarzschild BHs	29.3%
RR disks	23.8%
Schwarzschild stars	19.7%
Neutron stars	2.3%

Table 1: Upper limits for the efficiency η of different collision processes including Hawking's and Ellis' limit for the collision of two spherically symmetric black holes (Hawking & Ellis 1973). The maximum value for the collision of two RR disks is equal for scenario (A) and scenario (B), $\eta^{\mathrm{RR}}_{\max} = \eta^{\mathrm{DR}}_{\max} \approx 23.8\%$, see the last graph of Fig. 9 where $\eta^{\mathrm{F}}(1.954\ldots) = 0$.

4. Discussion

In this paper we have performed the analysis of collision processes in the spirit of equilibrium thermodynamics. Avoiding the solution of the full dynamical problem, we compared initial and final equilibrium configurations to obtain a "rough" picture of these processes. In this way we were able to calculate the energy loss by the emission of gravitational waves and to find conditions ("parameter relations") for the formation of final stars and disks.

The application of this method to collisions of perfect fluid stars and collisions of rigidly rotating disks of dust leads to restrictions of the initial parameters. It turned out that the formation of final stars/disks from stars/disks is only possible for a subset of the parameter space of the initial objects. Otherwise, the collision of spheres and disks would lead to other final states, e.g. to black holes.

Our main result is the numerical solution of the Einstein equations for the differentially rotating (DR) disk formed by the collision of two identical rigidly rotating (RR) disks with parallel angular momenta. We calculated the characteristic quantities of the final DR disk, as for example the rotation curve $\tilde{\Omega}(\tilde{\rho})$ as it depends on the centrifugal parameter μ of the initial RR disks. It turned out, that the angular velocity $\tilde{\Omega}$ is almost constant (as shown in Sec. 3.2.6, it is *strictly* constant in the Newtonian limit). Therefore, the simplified model of the formation of an RR disk from the collision of two RR disks as presented in Hennig & Neugebauer (2006), which has to allow frictional processes to reach constant angular velocity, turns out to be a good approximation to our present purely gravitational (frictionless) model (B).

For each of the studied collision scenarios, we calculated an upper limit for the energy of the emitted gravitational waves. A summary of the maximal efficiencies is given in table 1. The value $\eta_{\max} \approx 2.3\%$ for the collision of Neutron stars is relatively small compared to the

other examples. The reason is the restricted equation of state (completely degenerate ideal Fermi gas) that does not allow for strongly relativistic stars.

We would like to thank David Petroff for many valuable discussions. This work was supported by the Deutsche Forschungsgemeinschaft (DFG) through the SFB/TR7 "Gravitationswellenastronomie".

A. Potentials of the rigidly rotating disk of dust

For the numerical calculation of the DR disk that is formed by the collision of two RR disks we need some formulae for quantities of the RR disk of dust.

The coefficient V_0 in the four-velocity (27) as a function of the parameter μ can be calculated from a very rapidly converging series, cf. (Kleinwächter 1995),

$$\begin{aligned}\coth\frac{V_0}{2} &= -\frac{4}{\mu} + 0.0294938052100425142\mu + 5.4681333461446\cdot 10^{-6}\mu^3 \\ &\quad -1.07467432587\cdot 10^{-9}\mu^5 + 2.1127368\cdot 10^{-13}\mu^7 \\ &\quad -4.154\cdot 10^{-17}\mu^9 + \mathcal{O}(\mu^{11}).\end{aligned} \tag{A1}$$

The disk values ($\zeta = 0$, $\rho \le \rho_0$) of the metric functions U and a and the mass density σ are given by the equations

$$\mathrm{e}^{2U} = \mathrm{e}^{2V_0(\hat{\mu})} - \frac{\mu\rho^2}{2\rho_0^2}, \tag{A2}$$

$$(1+\Omega_0 a)\mathrm{e}^{2U} = \mathrm{e}^{V_0(\mu)}\mathrm{e}^{V_0(\hat{\mu})}, \tag{A3}$$

$$\sigma = -\frac{\Omega_0}{2\pi\mathrm{e}^{V_0(\mu)}}\frac{b_0'(\hat{\mu})}{\mathrm{e}^{V_0\hat{\mu}}}, \tag{A4}$$

with

$$\Omega_0 = \sqrt{\frac{\mu}{2}}\frac{\mathrm{e}^{V_0}}{\rho_0}, \quad b_0 = -\sqrt{1-\mathrm{e}^{4V_0}-4\Omega_0^2\rho_0^2}, \tag{A5}$$

cf. (Neugebauer & Meinel 1994). The notation $V_0(\hat{\mu})$, $b_0'(\hat{\mu})$ indicates that the argument μ in the parameter functions $V_0(\mu)$ and $b_0'(\mu)$ has to be replaced by $\hat{\mu} = (1-\rho^2/\rho_0^2)\mu$. $b_0'(\hat{\mu})$ means $\mathrm{d}b_0(\hat{\mu})/\mathrm{d}\hat{\mu}$.

REFERENCES

Anninos, P., Hobill, D., Seidel, E., Smarr, L., & Suen, W.-M. 1993, Phys. Rev. Lett., 71, 2851

Anninos, P., Hobill, D., Seidel, E., Smarr, L., & Suen, W.-M. 1995, Phys. Rev. Lett., 52, 2044

Anninos, P., & Brandt, S. 1998, Phys. Rev. Lett., 81, 508

Ansorg, M., & Meinel, R. 2000, Gen. Rel. Grav., 32, 1365

Ansorg, M. 2001, Gen. Rel. Grav., 33, 309

Ansorg, M., & Petroff, D. 2005, Phys. Rev. D, 72, 024019

Bardeen, J. M., & Wagoner, R. V. 1969, ApJ, 158, L65

Bardeen, J. M., & Wagoner, R. V. 1971, ApJ, 167, 359

Bardeen, J. M. 1973, in *Black Holes, Les astres occlus*, ed. DeWitt, C. & DeWitt, B., (Gordon and Breach Science Publishers, New York)

Beig, R., & Simon, W. 1992, Commun. Math. Phys., 144, 373

Eppley, K. 1975, Ph.D. thesis, Princeton University

Fiske, D. R., Baker, J. G., van Meter, R. R., Choi, & D.-I., Centrella, J. M. 2005, Phys. Rev. D, 71, 104036

Hawking, S. W., & G. F. R. Ellis, G. F. R. 1973, The large scale structure of space-time, Cambridge Monographs on Mathematical Physics, (Cambridge University Press)

Hennig, J., & Neugebauer, G. 2006, Phys. Rev. D, 74, 064025

Kleinwächter, A. 1995, Ph.D. thesis, Friedrich-Schiller-Universität Jena

Lindblom, L., & Masood-ul-Alam, A. K. M. 1994, Commun. Math. Phys., 162, 123

Löffler, F., Rezzolla, L., & Ansorg, M. 2006, Phys. Rev. D, 74, 104018

Misner, C. W., Thorne, K. S., & Wheeler, J. A 2002, Gravitation, (W. H. Freeman and Company, New York)

Neugebauer, G., & Meinel, R. 1993, ApJ., 414, L97

Neugebauer, G., & Meinel, R. 1994, Phys. Rev. Lett., 73, 2166

Neugebauer, G., & Meinel, R. 1995, Phys. Rev. Lett., 75, 3046

Neugebauer, G., Kleinwächter, A., & Meinel, R. 1996, Helv. Phys. Acta, 69, 472

Shapiro, S. L., & Teukolsky, S. A., Black Holes, White Dwarfs, and Neutron Stars — The Physics of Compact Objects, (John Wiley & Sons, New York)

Smarr, L., Čadež, A., DeWitt, B., & Eppley, K. 1976, Phys. Rev. D, 14, 2443

Sperhake, U., Kelly, B. , Laguna, P., Smith, K. L., & Schnetter, E. 2005, Phys. Rev. D, 71, 124042

Sperhake, U. 2006, gr-qc/0606079

Zlochower, Y., Baker, J. G., Campanelli, M., Lousto, C. O. 2005, Phys. Rev. D, 72, 024021